Catalysis Letters (2022) 152:361–371
https://doi.org/10.1007/s10562-021-03635-3

Catalytic Transfer Hydrogenation of Biomass-Derived 5-Hydroxymethylfurfural into 2,5-Dihydroxymethylfuran over Co/UiO-66-NH_2

Lu Wang[1,2] · Jianliang Zuo[1,2] · Qingtu Zhang[1,2] · Feng Peng[1,2] · Shengzhou Chen[1,2] · Zili Liu[1,2]

Received: 11 January 2021 / Accepted: 18 April 2021 / Published online: 2 May 2021

Abstract
A high-efficiency and low-cost Zr-based metal–organic frameworks loaded with Co catalyst for the catalytic transfer hydrogenation of biomass-derived 5-hydroxymethylfurfural (HMF) into 2,5-dihydroxymethylfuran (DHMF) through Meerwein–Ponndorf–Verley reduction was developed. A series of Co/UiO-66-NH_2 catalysts were synthesised by wet impregnation and reduction using the KBH_4 method and characterized by XRD, ICP-OES, XPS, SEM, TEM, BET and TPD techniques. As expected, $Co_{1.6}$/UiO-66-NH_2 displayed high catalytic transfer hydrogenation activity with 92.6% HMF conversion and 95.9% DHMF selectivity at a relatively mild reaction temperature (100 °C) in the presence of isopropanol that served as both hydrogen donor and reaction solvent. The highly dispersed Co species may effectively regulate the acid–base sites of the catalyst, which could be the main reason for the high hydrogenation activity.

Graphic Abstract

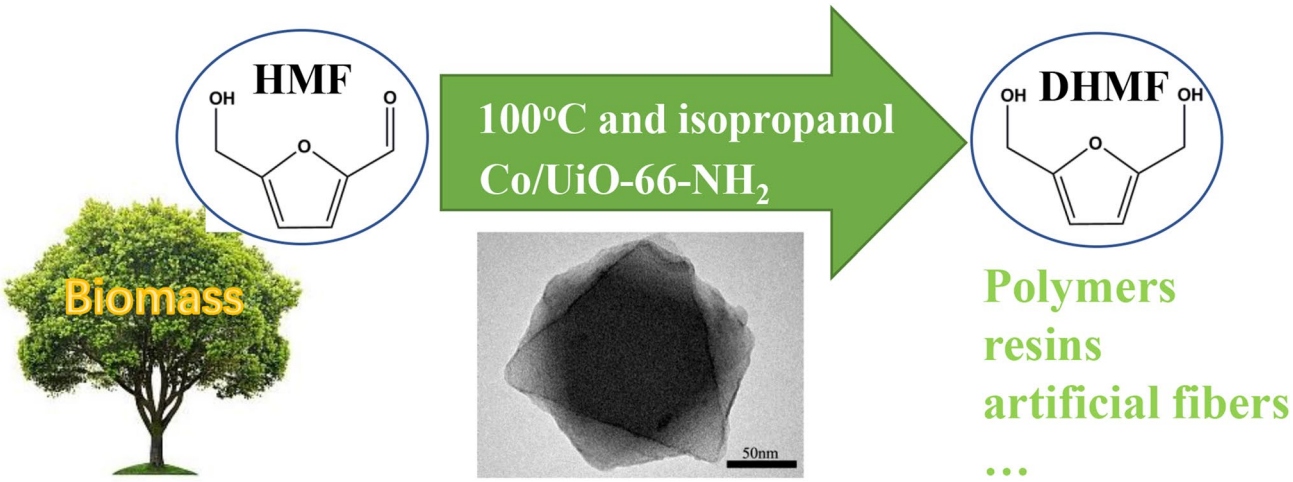

Keywords 5-Hydroxymethylfurfural · 2,5-Dihydroxymethylfuran · Metal–organic frameworks · Catalytic transfer hydrogenation

1 Introduction

The excessive consumption of fossil resources has led to serious energy crisis and environmental pollution. Therefore, it is necessary to develop renewable resources such as solar, wind and biomass [1, 2]. Biomass is a carbon-containing

✉ Jianliang Zuo
jlzuo@hotmail.com

✉ Zili Liu
gzdxlzl@163.com

Extended author information available on the last page of the article

renewable candidate that can be used as an alternative energy source and sustainable feedstock for future biofuels and chemicals while decreasing fossil fuel consumptions [3]. Among the biomass-derived chemicals, 5-hydroxymethylfurfural (HMF) is considered to be an important multifunctional intermediate that can be used to synthesise a variety of high-value derivatives such as 2,5-dihydroxymethylfuran (DHMF), 2,5-dihydroxymethyltetrahydrofuran (DHMTHF), 2,5-dimethylfuran (DMF), 2,5-furandicarboxylic acid (FDCA), 2,5-diformylfuran (DFF) and other chemicals, with potential applications in fuels, polymers, and solvents [4]. Among the furanic intermediates, DHMF— an alternative renewable polymer building blocks used in the synthesis of not only drugs but ethers, ketones, polymers, artificial fibers and resins—is obtained by the selective hydrogenation of HMF [5] and has aroused great interest of many researchers in recent years.

As we all know, HMF molecules contain three functional groups (aldehyde group, hydroxyl group and furan ring), which makes them chemically active. The conversion of HMF to DHMF involves only aldehyde group hydrogenation. Hence, the key issue is developing an appropriate catalytic system to ensure hydrogenation priority of the carbonyl group on HMF while avoiding further hydrogenation of the hydroxyl group and furan ring. Noble metal catalysts such as Pt/C [6], Au/Al_2O_3 [7], Ru/ZrO_2-SiO_2 [8], Ir/TiO_2 [9] and Pt/MCM-41 [10] have been widely studied and high conversion and selectivity have been obtained. However, there are some drawbacks that noble metal catalysts are expensive and H_2 used usually as hydrogen source, which are dangerous and expensive. From an economic and industrial perspective, it is imperative to develop inexpensive non-precious metal catalysts. Recently, some non-noble metal catalysts such as those based on Cu [11], Ni [12], Co [13] have been used in the selective hydrogenation of HMF to DHMF. Meanwhile, some new catalytic ways have been gradually developed, such as transfer hydrogenation [14, 15], photocatalytic hydrogenation [16], electrocatalytic hydrogenation [17], disproportionation reaction [18], and biocatalytic hydrogenation pathways [19], which offer promising alternatives to the conventional hydrogenation pathway that requiring additional molecular hydrogen. Among them, catalytic transfer hydrogenation is a promising way of hydrogenation, it usually involves the use of alcohol and acid as hydrogen donor and reaction medium, which improves the economy of transfer hydrogenation to a certain extent.

Metal–organic frameworks (MOFs) [20], a kind of porous crystalline material constructed from metal ions and organic ligands, with the advantages of large surface area, tunable pore sizes and controllable structures, have attracted widespread attention in heterogeneous catalysis, gas storage, separation process, chemical sensing, and many other fields [21]. Several studies on catalytic hydrogenation using MOF-based catalysts have been reported. Vasudeva et al. reported a Pd@UiO-66(Hf) core–shell catalyst that showed high activity for the selective transfer hydrogenation of vanillin to 2-methoxy-4-methylphenol under mild reaction conditions [22]. Chen et al. reported a Pd/MIL-101(Al)-NH_2 catalysts, which also had high activity under mild reaction conditions for the selective hydrogenation of HMF to DHMTHF with DHMF as an intermediate. The studies indicated that the observed high activity of DHMTHF is closely related to the cooperative effect between the metallic sites and the free amine moiety on the MOF [23]. MOF-based catalysts used above showed good activity, but noble metals were required. Therefore, it would be valuable to use non-noble metals for MOFs synthesis, so that they could be more affordable while still maintaining good activity. UiO-66-NH_2, a type of MOF with a large surface area, excellent chemical stability, thermal stability and structural stability in water, can be used as a suitable catalytic support [24]. Co could be used as active hydrogenation sites [25]. Herein we report a Co/UiO-66-NH_2 catalyst prepared by a simple impregnation-reduction method that showed highly selective transfer hydrogenation activity with 92.6% HMF conversion and 95.9% DHMF selectivity. The conversion was achieved using isopropanol as both the solvent and hydrogen donor under moderate reaction conditions, and the catalyst maintained good stability after five hydrogenation cycles. The Co/UIO-66-NH_2 catalyst holds great promise for use in the industrial production of DHMF.

2 Experimental

2.1 Chemicals and Materials

Zirconium chloride ($ZrCl_4$), 2-Aminoterephthalic acid (H_2ATA), Cobaltous chloride ($CoCl_2{\cdot}6H_2O$), Potassium borohydride (KBH_4), 5-Hydroxymethylfurfural (HMF), Benzoic acid, Pyridine and 2-Butanol were purchased from Shanghai Macklin Biochemical Co., Ltd. *N*, *N*-Dimethylformamide, Methanol, Ethanol, Isopropanol and 1-Butanol were purchased from Guangzhou Chemical Reagent Factory.

2.2 Catalyst Preparation

UiO-66-NH_2 was prepared according to a previously reported solvothermal method with slight modifications [26]. In a typical procedure, 1.119 g ($ZrCl_4$) and 0.87 g H_2ATA were dissolved in *N*, *N*-dimethylformamide (DMF) respectively, then the H_2ATA solution was poured into the $ZrCl_4$ solution. Acetic acid was added to the above solution and ultrasound for 20 min, the mixture solution was transferred to 100 mL Teflon-lined stainless-steel autoclaves. The autoclaves were sealed and heated at 120 °C for 24 h. After

cooling to the room temperature, the product was obtained by centrifugation, washed by DMF and ethanol three times respectively, and then soaked by methanol at 60 °C for 3 days to exchange the DMF solvents. The solid was dried at 70 °C under vacuum overnight.

Co/UIO-66-NH_2 was synthesized by the wet-impregnation and reduction using the KBH_4 method. The synthesis process was schematically shown in Scheme 1. In this case, a certain amount of $CoCl_2{\cdot}6H_2O$ (The amount of cobalt added is 5%, 10%, 15% and 20% according to the mass ratio of cobalt to precursor) was dissolved in 30 mL ethanol by sonication for 20 min, and 0.5 g UIO-66-NH_2 was dispersed into the above solution by sonication for another 20 min. Then the resulting mixture was stirred for 24 h at room temperature. The solid was separated by centrifugation and re-dispersed with deionized water. Then a freshly prepared 0.1 M KBH_4 (10 mL) solution was subsequently added and stirred for 3 h. The resulting solid powder was isolated by centrifugation, washed by deionized water three times, and dried at 70 °C under vacuum overnight. The final products were labeled as Co_x/UiO-66-NH_2 (x represents the actual cobalt loading determined by ICP-OES analysis).

2.3 Characterization

The X-ray diffraction patterns (XRD) of the prepared catalysts were determined by PANalytical PW3040/60 X-ray diffractometer, using CuKα radiation with a rate of 10°/min from 5° to 80°.

The elemental analysis was tested by Inductively Coupled Plasma Optical Emission Spectrometer (ICP-OES) on a Agilent 720ES instrument.

The surface areas were measured by N_2 adsorption–desorption method using a Micrometrics ASAP2460 instrument at − 196 °C, and calculated from the isotherms using the multipoint Brunauer–Emmett–Teller (BET) method.

The morphology, microstructure and the element distribution of samples were investigated by Field emission scanning electron microscopy (FESEM) (JSM-7001F) and Transmission electron microscopy (TEM) (JEM-2100F, JEOL).

The X-ray photoelectron spectroscopy (XPS) of catalysts were carried out on the Thermo XPS ESCALAB 250Xi spectrometer, equipped with a monochromatic Al Kα X-ray source (hm = 1486.8 eV).

The NH_3 temperature programmed desorption (NH_3-TPD) and CO_2 temperature programmed desorption (CO_2-TPD) were used to estimate the acidity and basicity of catalysts, using a TP-5076 catalyst analyzer. In each experiment, 0.1 g Catalyst was firstly pretreated for 2 h at 300 °C in He atmosphere. After cooling to 100 °C, the catalyst was exposed to NH_3/CO_2 atmosphere for 1 h. Then, the catalyst was purged with He atmosphere for 1 h to remove the physically adsorbed NH_3/CO_2. Finally, the desorption of NH_3/CO_2 was carried out in He atmosphere with a rate of 5 °C/min from 30 to 300 °C.

2.4 Activity Test and Product Analysis

Hydrogenation of HMF was carried out in a 100 mL stainless-steel autoclave with a pressure gauge and a magnetic stirrer. In a typical experiment, HMF (0.2 g), isopropanol (30 mL), toluene (0.05 g) and the catalyst (0.1 g) were added into the reactor. The reactor was purged with nitrogen gas at least 8 times to remove dissolved O_2 or air, then pressurized to demand N_2 pressure and heated to demand temperature with a mechanical stirring at a speed of 400 rpm. After completion of the reaction, the autoclave was cooled to room temperature quickly, and catalyst were separated by simple filtration. In a typical recycling test, the catalyst was separated from the reaction mixture by filtration after reaction, washed with ethanol three times, and then dried at 80 °C under vacuum for 12 h before reused in the next cycle. Qualitative and quantitative analysis of products were analyzed by GC–MS (Agilent 7890A + 5975) and GC (Agilent 6820) respectively. The contents of HMF, DHMF and others were determined by the internal standard curve method using toluene as an internal standard.

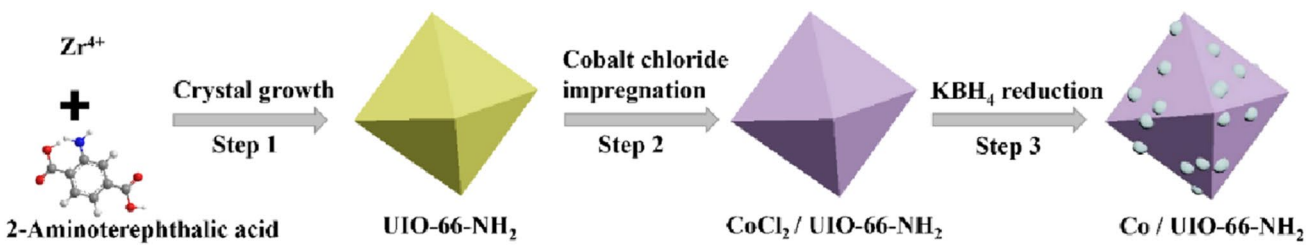

Scheme 1 Schematic illustration of process for preparing Co/UIO-66-NH_2 catalysts

3 Results and Discussion

3.1 Characterisation of Catalysts

Co/UiO-66-NH_2 was synthesised via wet-impregnation and subsequent potassium borohydride reduction method. In order to better understand the physicochemical properties of the catalysts, various characterisation methods were adopted, such as XRD, ICP-OES, SEM, TEM, XPS, BET and TPD. The results are summarised in the following sections.

The crystalline structures of the as-prepared samples were measured by XRD. The XRD patterns of UiO-66-NH_2 and Co_x/UiO-66-NH_2 were shown in Fig. 1. The characteristic peaks of UiO-66-NH_2 ($2\theta = 7.4°$, 8.6°) matched well with the previous report [27], exhibiting the excellent crystallinity, which proved the successful synthesis of UiO-66-NH_2. No significant loss of crystallinity was observed for the Co_x / UiO-66-NH_2 catalyst as compared with that of pristine UiO-66-NH_2, suggesting that the integrity of the UiO-66-NH_2 framework was maintained after immobilizing Co. No diffraction peaks attributable to Co species were found, which maybe due to the relatively low content and high dispersion of Co in UiO-66-NH_2. As can be seen from the ICP-OES test results (Table 1), the Co content of Co_x/UiO-66-NH_2 samples was low. Although the theoretical amount of added Co reached to 20%, the Co content in the composite was only 1.65%, indicating that it is difficult to introduce high-loading Co species into UIO-66-NH_2.

The morphology and structure of the catalysts were investigated by SEM and TEM, and the results were showed in Fig. 2. The UiO-66-NH_2 precursor (Fig. 2a) clearly showed octahedral structures with particle diameters of 200–400 nm, and the surface of the octahedra was glossy, which is in line with the literature [28]. The $Co_{1.6}$/UiO-66-NH_2 catalysts

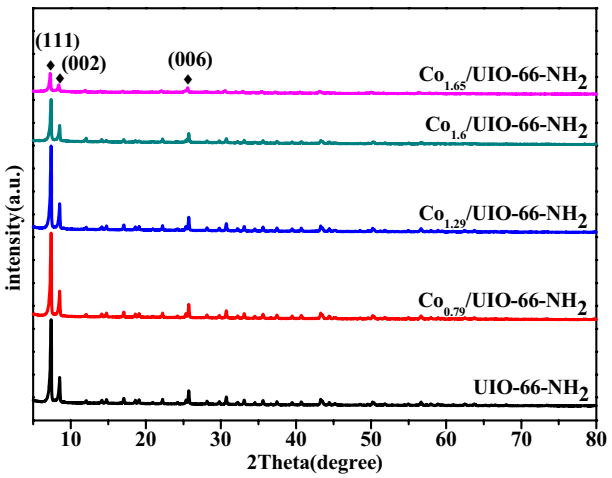

Fig. 1 XRD patterns of UiO-66-NH_2 and Co_x/UiO-66-NH_2 samples

Table 1 Physicochemical properties of UiO-66-NH_2 and Co_x/UiO-66-NH_2 catalysts

Entry	Samples	Co element content (wt%)[a]	Surface area (m^2/g)[b]
1	UIO-66-NH_2	0	715.69
2	Co_x/UIO-66-NH_2 (5 wt% Co starting amounts)	0.79	694.97
3	Co_x/UIO-66-NH_2 (10 wt% Co starting amounts)	1.29	671.10
4	Co_x/UIO-66-NH_2 (15 wt% Co starting amounts)	1.60	653.82
5	Co_x/UIO-66-NH_2 (20 wt% Co starting amounts)	1.65	630.56

[a]Determined by ICP-OES

[b]Measured using N_2 adsorption with the Brunauer–Emmett–Teller (BET) method

retained the octahedral structure, but the surface of the octahedra became rough (Fig. 2b). As seen in Fig. 2e, no obvious Co particles were observed. The EDS image (Fig. 2f) and element mapping image (Fig. 2g–j) revealed the existence of C, N, O, B, Zr and Co elements in the $Co_{1.6}$/UiO-66-NH_2 composite. It can be concluded that Co is low content and is uniformly dispersed on the catalyst, which verifies the previous results.

To further study the surface morphology of the as-prepared samples, N_2 adsorption–desorption isotherm experiments were applied. The isotherm curves and surface area results were determined by BET treatment of UIO-66-NH_2 and Co_x/UIO-66-NH_2, as shown in Fig. 3 and Table 1. The isotherm curves of the as-obtained samples demonstrated typical type-I isotherms for microporous adsorption. Compared to UiO-66-NH_2, with increased Co content, the BET surface area of the Co_x/UIO-66-NH_2 series samples decreased.

The surface chemical composition and elemental distribution in UiO-66-NH_2 and $Co_{1.6}$/UiO-66-NH_2 samples were ascertained by XPS analysis, with the results shown in Fig. 4. The XPS survey scan (Fig. 4a) showed that the $Co_{1.6}$/UiO-66-NH_2 catalyst was composed of Co, Zr, C, N, O, and B elements. Figure 4b showed the curves of the Zr 3d region, characteristic peaks at binding energies of 182.55 eV and 184.95 eV corresponding to the Zr $3d_{5/2}$ and Zr $3d_{3/2}$ states of Zr^{4+} in $Co_{1.6}$/UiO-66-NH_2, respectively, which shift to lower binding energies compared to those of UiO-66-NH_2 [24]. As shown in Fig. 4c, the spectrum shows four weak Co 2p peaks. The peaks at binding energies of 781.53 eV and 797.33 eV are attributed to Co $2p_{3/2}$ and Co $2p_{1/2}$ respectively. The results showed that Co species existed in the

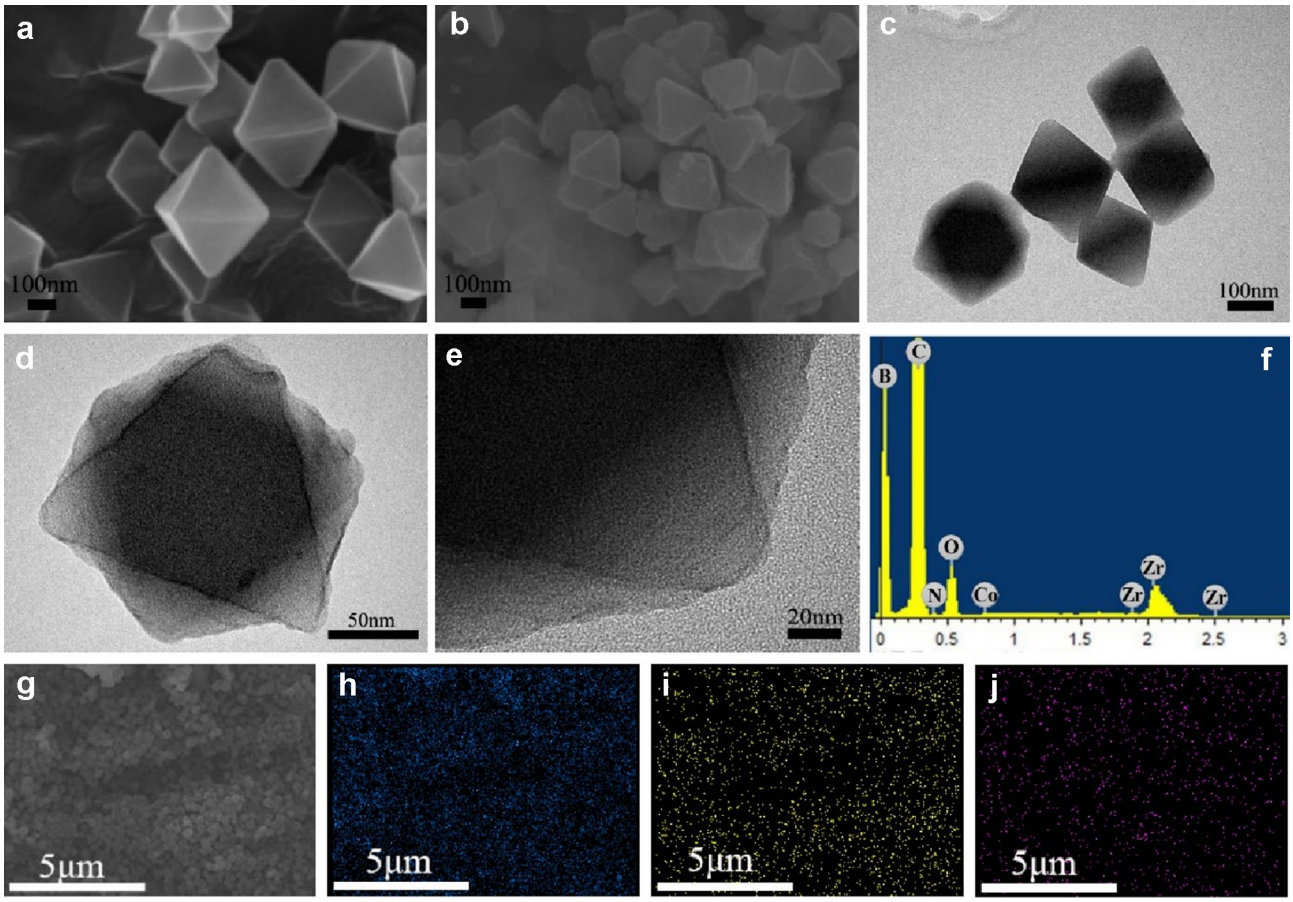

Fig. 2 SEM images of UiO-66-NH_2 (**a**) and $Co_{1.6}$/UiO-66-NH_2 (**b**); TEM images of UiO-66-NH_2 (**c**) and $Co_{1.6}$/UiO-66-NH_2 (**d**, **e**) with different magnification; EDS spectrum (**f**) of $Co_{1.6}$/UiO-66-NH_2; SEM image of $Co_{1.6}$/UiO-66-NH_2 (**g**) and element mapping of Zr (**h**), B (**i**), Co (**j**)

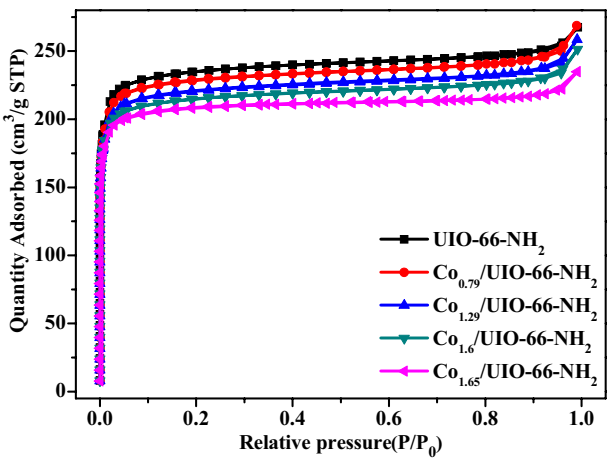

Fig. 3 The N_2 adsorption–desorption isotherms of UiO-66-NH_2 and Co_x/UiO-66-NH_2 samples

elemental state as Co–B alloy or Co^0 and oxidation state, and the detected Co oxide species can be attributed to oxidation during the preparation of the catalyst. The Co–B alloy existed in Co/UIO-66-NH_2 catalyst, wherein the combination of the transition metal Co with the metalloid atom B changed the intrinsic electronic states of the transition metal (electronic effect), thus improving the catalytic performance [29]. The atomic ratio of Co was 1.22% from the XPS analysis, which certified the low Co content. The spectrum of B1s is shown in Fig. 4d, there are two characteristic peaks at 192.53 eV and 196.58 eV, corresponding to B–Co and B–O respectively [30, 31]. As shown in Fig. 4e, the N 1s XPS spectrum of $Co_{1.6}$/UiO-66-NH_2 located at 399.40 eV. No significant difference was observed compared with that of UiO-66-NH_2 [32], suggesting that the -NH_2 groups on the organic linkers could be retained during the synthesis and they did not coordinate with the Co metal ions. Figure 4f displayed the C 1s spectra of UiO-66-NH_2, the fitting peaks at 284.68 eV, 285.16 eV and 288.75 eV were corresponded to the C=C, C–N bonds and O–C=O group of H_2ATA, respectively [27]. For $Co_{1.6}$/UiO-66-NH_2, deconvoluted C1s peaks were observed at 284.60 eV, 285.23 eV and 288.81 eV, respectively.

As can be seen from Fig. 5 and Table 2, the acid–base properties of the catalyst were studied. Figure 5a showed the

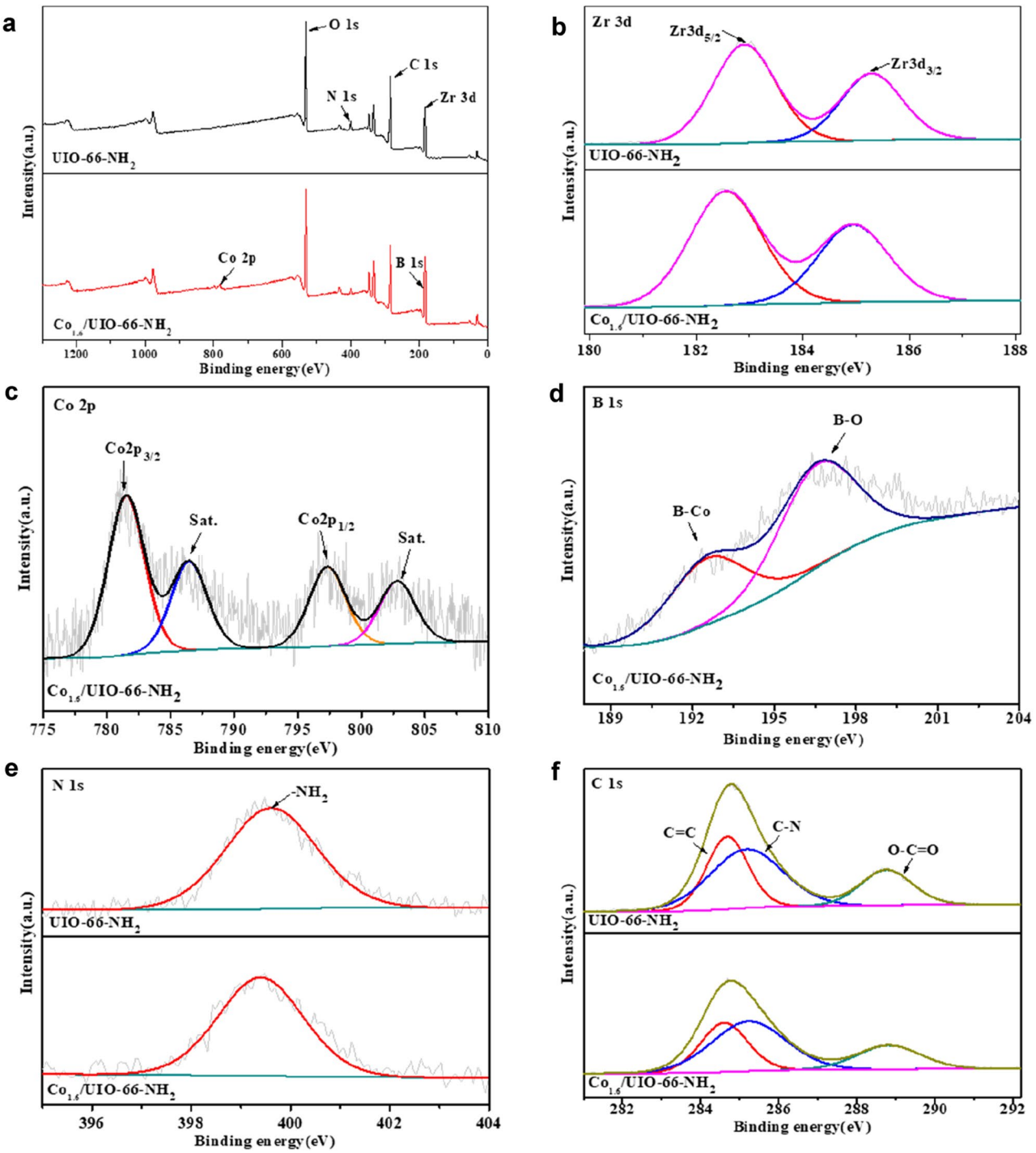

Fig. 4 XPS spectra of UiO-66-NH_2 and $Co_{1.6}$/UiO-66-NH_2 sample: **a** survey, **b** Zr 3d, **c** Co 2p, **d** B 1s, **e** N 1s and **f** C 1s

CO_2-TPD profiles of UiO-66-NH_2 and $Co_{1.6}$/UiO-66-NH_2, which indicate that both have base sites, and Table 2 showed that the $Co_{1.6}$/UiO-66-NH_2 had more base sites than UiO-66-NH_2. Figure 5b showed the NH_3-TPD profiles of UiO-66-NH_2 and $Co_{1.6}$/UiO-66-NH_2, which show that they both have acid sites, Conversely, Table 2 showed that the $Co_{1.6}$/UiO-66-NH_2 had fewer acid sites than UiO-66-NH_2. From the above results, it can be concluded that UiO-66-NH_2 and $Co_{1.6}$/UiO-66-NH_2 are amphoteric catalysts with both acidic and basic properties. And the addition of cobalt affected the acid sites and base sites of the catalyst.

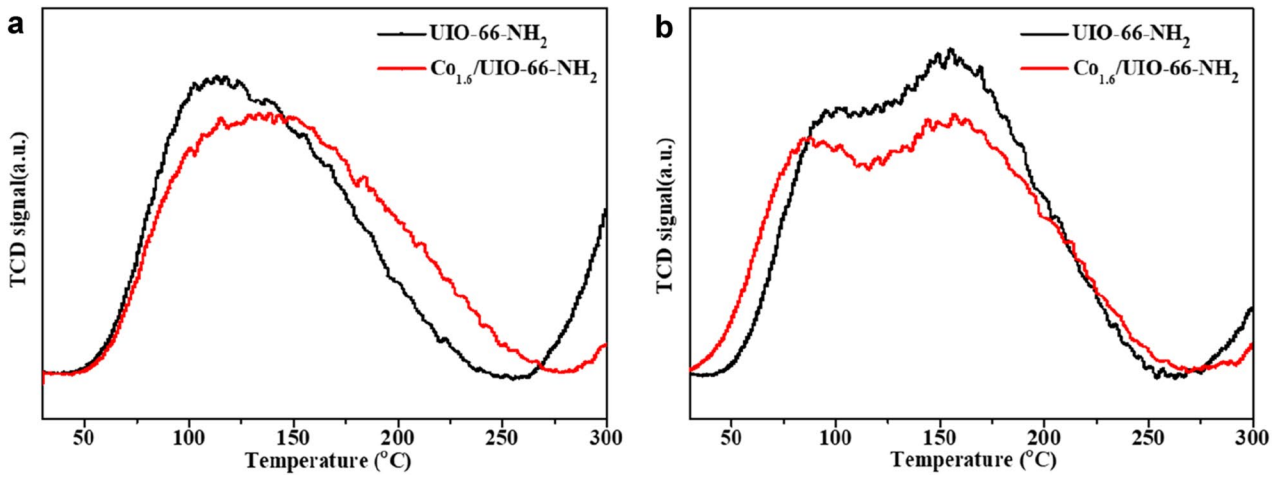

Fig. 5 CO_2-TPD profiles (**a**) and NH_3-TPD profiles (**b**) of UiO-66-NH_2 and $Co_{1.6}$/UiO-66-NH_2

Table 2 The acid–base properties of UIO-66-NH_2 and $Co_{1.6}$/UIO-66-NH_2

Entry	Samples	Acid sites (μmol/g)[a]	Base sites (μmol/g)[b]
1	UiO-66-NH_2	452.8	132.2
2	$Co_{1.6}$/UiO-66-NH_2	428.1	160.7

[a]Acid sites were calculated by the profile of NH_3-TPD

[b]Base sites were calculated by the profile of CO_2-TPD

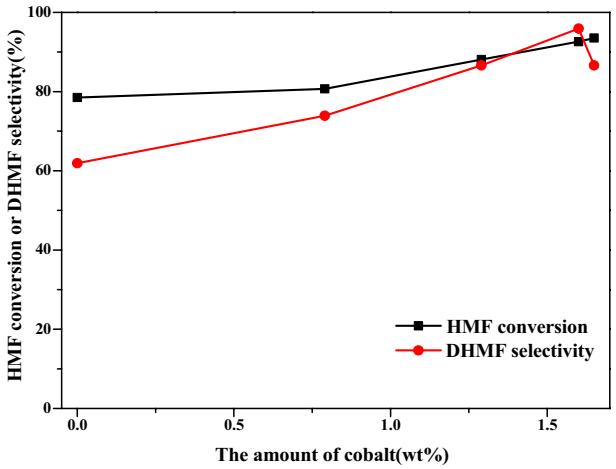

Fig. 6 MPV reduction of HMF into DHMF over various catalysts. Reaction conditions: 0.2 g HMF, 0.1 g catalyst, 0.05 g toluene, 30 mL isopropanol, 100 °C, 4 h

3.2 Catalytic Activities of HMF Transfer Hydrogenation

In the earlier stage study, the activities of different catalysts were investigated in isopropanol at 100 °C for 4 h, wherein isopropanol was used as both hydrogen donor and reaction medium. As shown in Fig. 6, UIO-66-NH_2 showed moderate activity with 78.5% HMF conversion and 61.9% DHMF selectivity. With increased Co loading, the catalytic activity increased significantly. The $Co_{1.6}$/UIO-66-NH_2 catalyst exhibited the highest activity with 92.6% conversion of HMF and 95.9% selectivity for DHMF. A further increase in Co loading resulted in decreased activity, and the $Co_{1.65}$/UIO-66-NH_2 catalyst showed 93.5% HMF conversion and 86.6% DHMF selectivity. Excessive Co may aggregate, leading to a decrease in the selectivity. The excellent catalytic performance of $Co_{1.6}$/UIO-66-NH_2 means appropriate Co loading facilitates the transfer hydrogenation of HMF [25, 33]. Therefore, $Co_{1.6}$/UIO-66-NH_2 was selected as the optimal catalyst for the preparation of DHMF from HMF.

The effects of the alcohol type, reaction temperature, reaction pressure and reaction time on the selective conversion of HMF to DHMF over the $Co_{1.6}$/UIO-66-NH_2 catalyst were studied. As shown in Fig. 7a, we found that higher catalytic activity was achieved in isopropanol than in methanol, ethanol, 1-butanol and 2-butanol. HMF conversion and DHMF selectivity are closely connected to the reduction potentials (RPs) of alcohols, in the following order: methanol (130.1 kJ/mol) > ethanol (85.4 kJ/mol) > 1-butanol (79.7 kJ/mol) > isopropanol (70.0 kJ/mol) ≈ 2-butanol (69.3 kJ/mol) [34]. Among these, methanol has the highest RP, and hence, it has the poorest capacity as a hydrogen donor with no DHMF generated. It is not difficult to found that the secondary alcohols, such as isopropanol and 2-butanol are more effective than the above primary alcohols in MPV reduction due to their low RPs.

The effect of reaction temperature on the MPV reduction of HMF into DHMF was studied at 2 MPa for a reaction time of 4 h (Fig. 7b). As the reaction temperature increased from 80 to 100 °C, the HMF conversion increased from 54.6

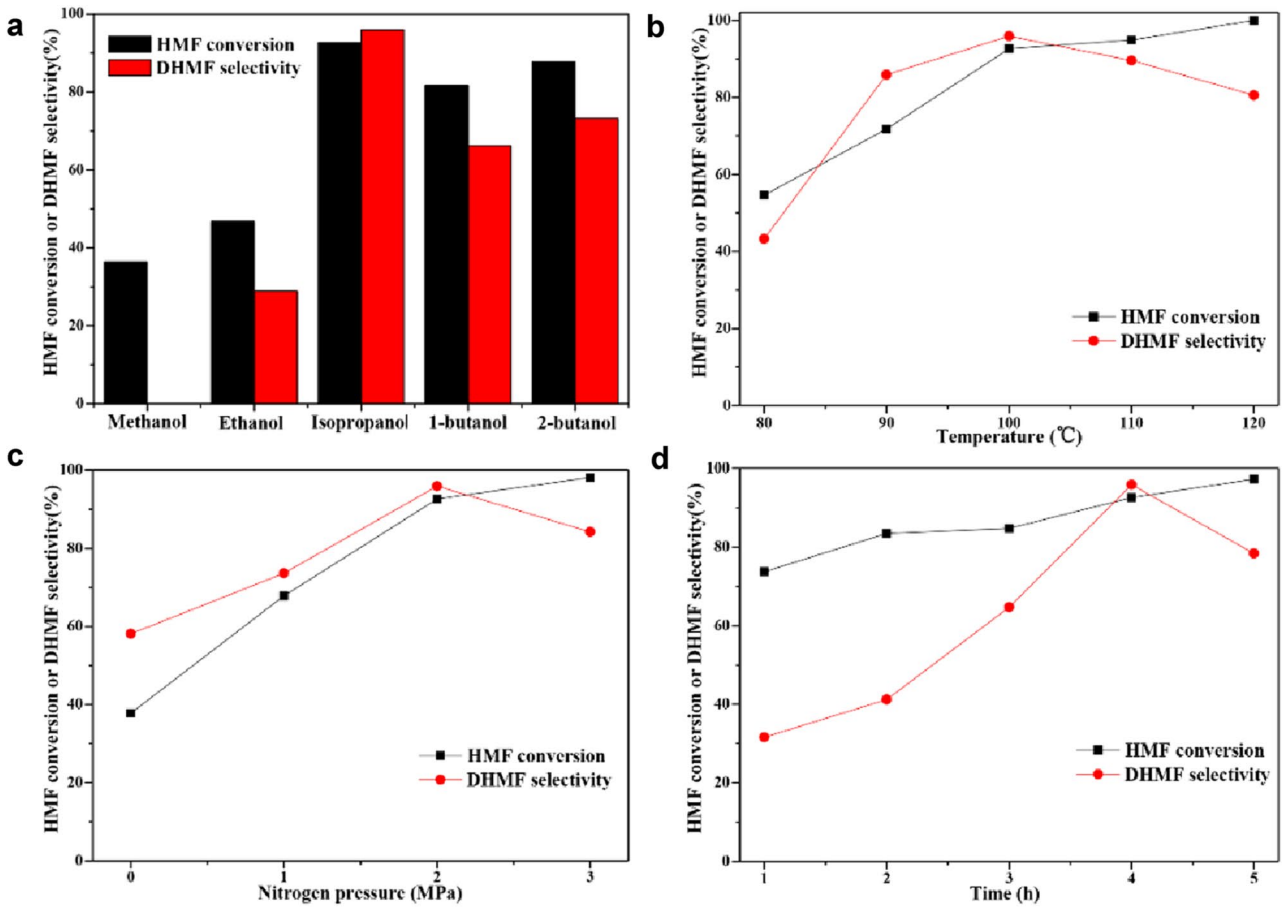

Fig. 7 Effects of alcohol type (**a**), reaction temperature (**b**), reaction pressure (**c**) and reaction time (**d**) on the MPV reduction of HMF into DHMF over $Co_{1.6}$/UIO-66-NH_2. Reaction conditions: (a) 0.2 g HMF, 0.1 g catalyst, 30 mL alcohol, 2 MPa N_2, 100 °C, 4 h; (b) 0.2 g HMF, 0.1 g catalyst, 30 mL isopropanol, 2 MPa N_2, 4 h; (c) 0.2 g HMF, 0.1 g catalyst, 30 mL isopropanol, N_2, 100 °C, 4 h; (d) 0.2 g HMF, 0.1 g catalyst, 30 mL isopropanol, 2 MPa N_2, 100 °C

to 92.6% and the DHMF selectivity increased from 43.3 to 95.9%. With a further increase in the temperature, the HMF conversion increased, but the selectivity decreased, leading to the formation of more by-products.

The catalytic activity of $Co_{1.6}$/UIO-66-NH_2 was also related to the reaction pressure (Fig. 7c). As the reaction pressure increased from 0 to 2 MPa at 100 °C for a reaction time of 4 h, the HMF conversion and DHMF selectivity increased sharply from 37.8 to 92.6% and from 58.1 to 95.9%, respectively. However, at 3 MPa, the DHMF selectivity decreased to 84.2%, despite the HMF conversion increasing to 98.1%. Therefore, a pressure of 2 MPa is considered to be optimal pressure for achieving high HMF conversion and high DHMF selectivity.

Next, we studied the effect of the reaction time at 100 °C and 2 MPa (Fig. 7d). As the reaction time increased from 1 to 4 h, the HMF conversion and DHMF selectivity increased from 73.7 to 92.6% and from 31.6 to 95.9%, respectively. When the reaction lasted for 5 h, the conversion continued to increase while the selectivity decreased to 78.4%, indicating byproduct formation after long reaction times.

In summary, the $Co_{1.6}$/UIO-66-NH_2 catalyst achieved the best activity with 92.6% HMF conversion and 95.9% DHMF selectivity in catalytic transfer hydrogenation at a mild reaction temperature (100 °C) in the presence of isopropanol that served as both hydrogen donor and reaction solvent. For comparison, the catalyst activity in recent reports on the transfer hydrogenation of HMF to DHMF is summarised in Table 3. It can be seen that the catalyst synthesised in this study can achieve excellent catalytic activity at lower temperature.

3.3 Catalytic Recyclability

The stability of catalyst is very important in heterogeneous catalysis, and it is of great significance in reducing the cost of product synthesis. Therefore, we investigated the stability of the $Co_{1.6}$/UIO-66-NH_2 catalyst at 100 °C and 2 MPa N_2 for 4 h (Fig. 8). After the reaction, the catalyst was recovered through filtration, washed with ethanol, and dried for the next cycle. When $Co_{1.6}$/UIO-66-NH_2 was reused 5 recycles, HMF conversion and DHMF selectivity were still achieved

Table 3 Comparison of the selectivity of DHMF and conversion of the HMF hydrogenolysis over various Zr-base catalysts

Catalyst	Temp. (°C)	Time (h)	Hydrogen donor	HMF Conv. (%)	DHMF Select. (%)	Refs.
$ZrO(OH)_2$	150	2.5	Ethanol	94.1	88.9	[35]
Magnetic zirconium hydroxides (MZHs)	150	5	2-Butanol	98.4	89.6	[33]
Magnetic zirconium–cyanuric acid coordination polymer (MZCCP)	140	5	2-Butanol	98.7	93.4	[36]
ZrBa-SBA	150	2.5	Isopropanol	98.3	92.2	[37]
Amorphous and mesoporous zirconium phosphonate catalyst (Zr-DTMP)	140	3	2-Butanol	100	96.5	[38]
$Co_{1.6}$/UIO-66-NH_2	100	4	Isopropanol	92.6	95.9	Our work

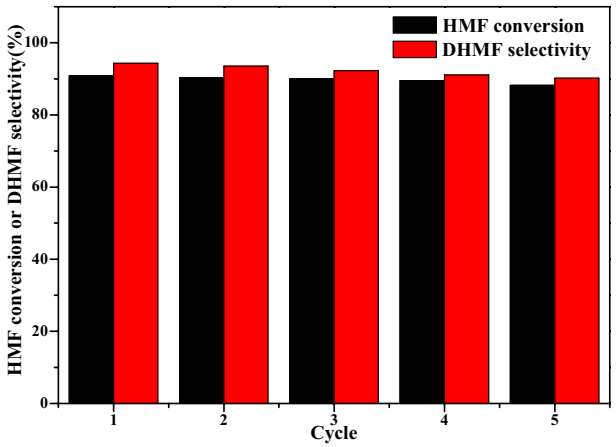

Fig. 8 Catalytic recycling of $Co_{1.6}$/UIO-66-NH_2 for the MPV reduction of HMF to DHMF. Reaction conditions: 0.2 g HMF, 0.1 g catalyst, 0.05 g toluene, 30 mL isopropanol, 100 °C, 4 h

to 88.2% and 90.2%, respectively, indicating that the catalyst had excellent stability. Furthermore, the recovered $Co_{1.6}$/UIO-66-NH_2 catalyst after 5 recycles was characterized by XRD and SEM (Fig. 9). Obviously, compared with the fresh $Co_{1.6}$/UIO-66-NH_2, the physicochemical properties and structural properties of the catalyst were almost unchanged, which further indicated that the $Co_{1.6}$/UIO-66-NH_2 catalyst in this study was very stable.

3.4 Plausible Mechanism for MPV Reduction of HMF into DHMF over $Co_{1.6}$/UIO-66-NH_2

In order to better understand the role of the catalyst in the MPV reduction reaction, benzoic acid and pyridine were added into the reaction system as poisoning additives [39]. It was observed that the addition of pyridine sharply reduced the conversion of HMF and the selectivity of DHMF, indicating that the $Co_{1.6}$/UIO-66-NH_2 catalytic MPV reduction reaction was closely related to the acid sites at the catalyst surface. However, in the presence of benzoic acid, the conversion of HMF decreased and no DHMF was produced. It can be found that both acid and base sites have significant effects on the catalytic activity of $Co_{1.6}$/UIO-66-NH_2, but the poisoning of base sites had a greater impact on the catalytic

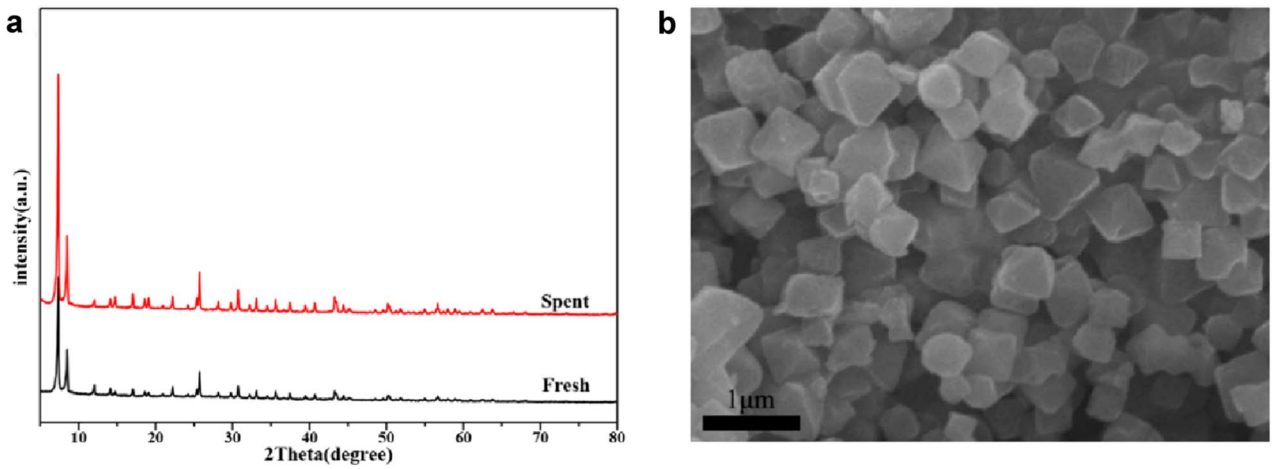

Fig. 9 XRD pattern (**a**) and SEM image (**b**) of the spent $Co_{1.6}$/UIO-66-NH_2

Table 4 Effects of additives on the MPV reduction of HMF into DHMF over $Co_{1.6}$/UIO-66-NH_2

Entry	Additive	HMF conversion (%)	DHMF selectivity (%)
1	Blank	90.8	94.3
2	Pyridine[a]	69.7	49.5
3	Benzoic acid[a]	45.8	0

Reaction conditions: 0.2 g HMF, 0.1 g catalyst, 0.05 g toluene, 30 mL isopropanol,100 °C, 4 h

[a]The amount of additive was 0.1 g

performance than that of acid sites. This trend is consistent with the TPD results describe above (Table 4).

4 Conclusions

We reported a kind of acid–base bifunctional catalyst—Co/Zr-based MOFs—that showed significant catalytic activity in direct hydrogen transfer from biological carbonyl compounds for the formation of valuable and highly selective alcohols in the MPV reaction. $Co_{1.6}$/UIO-66-NH_2 achieved high activity with 92.6% conversion of HMF and 95.9% selectivity of DHMF in the presence of isopropanol under mild reaction conditions (100 °C for 4 h). Furthermore, the catalyst had no significant loss of catalytic activity after five cycles, showing good chemical stability. We believe that MOFs based catalysts show great potential for the catalytic transfer hydrogenation reaction of other biomass-derived molecules.

Acknowledgements The financial supports provided by the National Natural Science Foundation of China (22005070, 21676060) and Scientific Research Project of Guangzhou Municipal Colleges and Universities (202032855).

References

1. Luterbacher JS, Rand JM, Alonso DM, Han J, Youngquist JT, Maravelias CT, Pfleger BF, Dumesic JA (2014) Science 343:277–280
2. Román-Leshkov Y, Barrett CJ, Liu ZY, Dumesic JA (2007) Nature 447:982–985
3. Melero JA, Iglesias J, Garcia A (2012) Energy Environ Sci 5:7393
4. Zhang L, Xi G, Chen Z, Qi Z, Wang X (2017) Chem Eng J 307:877–883
5. Gelmini A, Albonetti S, Cavani F, Cesari C, Lolli A, Zanotti V, Mazzoni R (2016) Appl Catal B Environ 180:38–43
6. Balakrishnan M, Sacia ER, Bell AT (2012) Green Chem 14:1626
7. Ohyama J, Esaki A, Yamamoto Y, Arai S, Satsuma A (2013) RSC Adv 3:1033–1036
8. Chen JZ, Lu F, Zhang JJ, Yu WQ, Wang F, Gao J, Xu J (2013) ChemCatChem 5:2822–2826
9. Cai H, Li C, Wang A, Zhang T (2014) Catal Today 234:59–65
10. Chatterjee M, Takayuki I, Hajime K (2014) Green Chem 16:4734–4739
11. Chen BF, Li FB, Huang ZJ, Yuan GQ (2017) Appl Catal B Environ 200:192–199
12. Yu LL, He L, Chen J, Zheng JW, Ye LM, Lin HQ, Yuan YZ (2015) ChemCatChem 7:1701–1707
13. Wang GH, Hilgert J, Richter FH, Wang F, Bongard HJ, Spliethoff B, Weidenthaler C, Schuth F (2014) Nat Mater 13:293–300
14. Li H, Fang Z, He J, Yang S (2017) ChemSusChem 10:681–686
15. Wang T, Zhang JH, Xie WX, Tang YJ, Guo DL, Ni YH (2017) Catalysts 7:92
16. Guo YY, Chen JZ (2016) RSC Adv 6:101968–101973
17. Roylance JJ, Kim TW, Choi KS (2016) ACS Catal 6:1840–1847
18. Li G, Sun Z, Yan Y, Zhang Y, Tang Y (2016) ChemSusChem 9:1–6
19. He YC, Ding Y, Ma CL, Di JH, Jiang CX, Li A (2017) Green Chem 19:3844–3850
20. Stock N, Biswas S (2012) Chem Rev 112:933–969
21. Cui YJ, Li B, He HJ, Zhou W, Chen BL, Qian GD (2016) ChemInform 49:483–493
22. Bakuru VR, Davis D, Kalidindi SB (2019) Dalton Trans 48:8573–8577
23. Chen J, Liu R, Guo Y, Chen L, Gao H (2014) ACS Catal 5:722–733
24. Shen L, Liang S, Wu W, Liang R, Wu L (2013) J Mater Chem A 1:11473–11482
25. Li D, Liu Q, Zhu C, Wang H, Cui C, Wang C, Ma L (2019) J Energy Chem 30:34–41
26. Yuan LP, Yin LS, Cao SW, Xu GS, Li CH, Xue C (2015) Appl Catal B Environ 168–169:572–576
27. Shen L, Wu W, Liang R, Lin R, Wu L (2013) Nanoscale 5:9374–9382
28. Xu J, He S, Zhang HL, Huang JC, Lin HX, Wang XX, Long JL (2015) J Mater Chem A 3:24261–24271
29. Li F, Li J, Chen LY, Dong YM, Xie P, Li QM (2020) Int J Hydrog Energy 45:32145–32156
30. Sukanya R, Chen SM (2020) J Colloid Interface Sci 580:318–331
31. Glavee GN, Klabunde KJ, Sorensen CM, Hadjipanayis GC (1993) Langmuir 9:162–169
32. Shen L, Liang S, Wu W, Liang R, Wu L (2013) Dalton Trans 42:13649–13657
33. Hu L, Yang M, Xu N, Xu J, Zhou S, Chu X, Zhao Y (2017) Korean J Chem Eng 35:99–109
34. Van der Waal JC, Kunkeler PJ, Tan K, Van Bekkum H (1998) J Catal 173:74–83
35. Hao W, Li W, Tang X, Zeng X, Sun Y, Liu S, Lin L (2015) Green Chem 18:1080–1088
36. Hu L, Li T, Xu J, He A, Tang X, Chu X, Xu J (2018) Chem Eng J 352:110–119
37. Wei J, Cao X, Wang T, Liu H, Tang X, Zeng X, Sun Y, Lei T, Liu S, Lin L (2018) Catal Sci Technol 8:4474–4484
38. Hu L, Li N, Dai X, Guo Y, Jiang Y, He A, Xu J (2019) J Energy Chem 37:82–92
39. Zhou SH, Dai FL, Chen YA, Dang C, Zhang CZ, Liu DT, Qi HS (2019) Green Chem 21:1421

Authors and Affiliations

Lu Wang[1,2] · Jianliang Zuo[1,2] · Qingtu Zhang[1,2] · Feng Peng[1,2] · Shengzhou Chen[1,2] · Zili Liu[1,2]

[1] School of Chemistry and Chemical Engineering, Guangzhou University, Guangzhou 510006, Guangdong, China

[2] Guangzhou Key Laboratory for New Energy and Green Catalysis, Guangzhou 510006, Guangdong, China